

1

2

### 3 Formation and Spontaneous Long-Term Repatterning of Headless Planarian Flatworms

4

5

6 Johanna Bischof\*, Jennifer V. LaPalme\*, Kelsie A. Miller, Junji Morokuma, Katherine B. Williams,  
7 Chris Fields, and Michael Levin<sup>#</sup>

8

9

10 Allen Discovery Center

11 Tufts University

12 Medford, MA

13

14 \* Authors contributed equally to the work

15 # Author for correspondence:

16 Email: [michael.levin@tufts.edu](mailto:michael.levin@tufts.edu)

17 Tel.: (617) 627-6161

18

19

20 **Keywords:** planarian, regeneration, remodeling, morphallaxis, ERK signaling, long-term

21

22 **Running title:** Long-term polarity remodeling

23

24     **Abstract**

25                 Regeneration requires the production of large numbers of new cells, and thus cell division  
26     regulators, particularly ERK signaling, are critical in regulating this process. In the highly regenerative  
27     planarian flatworm, questions remain as to whether ERK signaling controls overall regeneration or plays  
28     a head-specific role. Here we show that ERK inhibition in the 3 days following amputation delays  
29     regeneration, but that all tissues except the head can overcome this inhibition, resulting in headless  
30     regenerates. This prevention of head regeneration happens to a different degree along the anterior-  
31     posterior axis, with very anterior wounds regenerating heads even under ERK inhibition. Remarkably, 4 to  
32     18 weeks after injury, the headless animals induced by ERK inhibition remodel to regain single-headed  
33     morphology, in the absence of further injury, in a process driven by Wnt/β-catenin signaling. Interestingly,  
34     headless animals are likely to exhibit unstable axial polarity, and cutting or fissioning prior to remodeling  
35     can result in body-wide reversal of anterior-posterior polarity. Our data reveal new aspects of how ERK  
36     signaling regulates regeneration in planaria and show anatomical remodeling on very long timescales.

37 **Introduction**

38 Following injury or disease, some animals are capable of replacing lost structures <sup>1</sup>. Such  
39 regenerative processes require the production of new cells, in most systems achieved through the  
40 activation of stem cells <sup>2,3</sup>. ERK/MAP Kinase signaling is one of the crucial regulators of cell division <sup>4</sup> and  
41 has been shown to play an important role in many model systems of regeneration <sup>5,6</sup>. In the highly  
42 regenerative planarian flatworm, ERK phosphorylation is one of the first responses to injury, detectable  
43 15 min after cutting <sup>7</sup>. ERK signaling has been argued to be important in planaria for overall regeneration  
44 <sup>7</sup>, to play a role in allowing differentiation <sup>6</sup>, to activate stem cell subpopulations <sup>8</sup> and to play a head-  
45 specific role <sup>9</sup>. Several studies have shown that ERK inhibition immediately following amputation leads to  
46 the formation of headless animals <sup>6,7,9</sup>.

47 The variety of regenerative activities that ERK signaling has been reported to mediate suggests  
48 that ERK signaling exists in a complex milieu of different signaling factors that interact in ways that are  
49 only beginning to be understood <sup>10</sup>. For example, Follistatin, a secreted inhibitor of activin signaling, was  
50 recently shown to be conditionally required for head regeneration in planaria, dependent on the  
51 underlying Wnt signaling environment at the injury site <sup>11,12</sup>, illustrating that the complex factors that  
52 regulate regeneration are interacting in a dynamic and spatial distinct manner that remains to be fully  
53 described.

54 Planarian regeneration is a complex and highly regulated process, that is also very dynamic, with  
55 planarians completing regeneration within 7-10 days, regardless of whether they are forming a wild-type  
56 anatomy or heteromorphoses, such as 2-headed or headless morphologies <sup>13</sup>. Even in the absence of  
57 major wounding events, planaria continuously adjust their size to changes in nutritional availability by  
58 shrinking and growing to maintain correct proportions <sup>14,15</sup>. Underpinning this size adaptation is the  
59 constant cell turnover which occurs around every 30 days, the longest regenerative timeframe that has  
60 been described in planaria <sup>16,17</sup>. Most regeneration studies in planaria stop characterizing regeneration  
61 effects around 14 days after injury and little work has explored repatterning and changes to morphology  
62 on longer timescales. Planarian regenerative outcomes, such as the headless worms induced by ERK  
63 inhibition, have previously been assumed to be permanent <sup>7</sup>.

64 Here we show that ERK inhibition for the first 3 days after amputation specifically inhibits head  
65 regeneration, while other tissues, such as the tail, can fully regenerate after ERK inhibition. This effect of  
66 ERK inhibition on regenerative outcomes is dependent on the underlying signaling environment, with

67 head regeneration still occurring following ERK inhibition in the very anterior regions of the animal.  
68 Remarkably, we found that without any further external manipulation, the headless animals generated  
69 through ERK inhibition do not permanently remain headless but spontaneously begin to repattern to a  
70 wild-type anatomy anywhere between 4 and 18 weeks after their original formation. This repatterning  
71 occurs after the regeneration-driven remodeling is complete and is regulated by Wnt/β-catenin signaling.  
72 Finally, we show that headless animals appear to lack stable axial polarity, as their anterior-posterior axis  
73 can become reversed following bisection or fissioning, with a head forming from a posterior blastema.  
74 Thus, our findings reveal that *D. japonica* can undergo spontaneous repatterning to overcome the  
75 headless morphology and remodel tissue long after regeneration is completed, indicative of remodeling  
76 processes controlling morphology on longer timescales than previously known.

77 **Result and Discussion**

78

79 *Short term ERK inhibition selectively blocks regeneration of anterior tissue*

80 ERK signaling has been shown to play a role in controlling regeneration in both *Schmidtea mediteranea* and *Dugesia japonica* planarians<sup>6,7,9</sup>. Therefore, with the goal of exploring the effect of a  
81 short-term inhibition of regeneration on overall regenerative outcomes in *Dugesia japonica*, we treated  
82 pre-tail fragments (with both anterior and posterior wounds requiring regeneration), for 3 days with the  
83 highly specific and efficient ERK inhibitor U0126<sup>7</sup> (Figure 1A). Following this 3-day treatment, we found  
84 that 98% of fragments regenerated as headless animals within 7 days (Figure 1B), lacking both external  
85 head structures and a brain (Figure 1B). The regeneration was determined to be complete by closure of  
86 the wound, pigmentation of any blastema tissue and formation of a stable morphology. This recapitulates  
87 previous reports that various ERK inhibition methods all result in headless animals<sup>6,7,9</sup>.

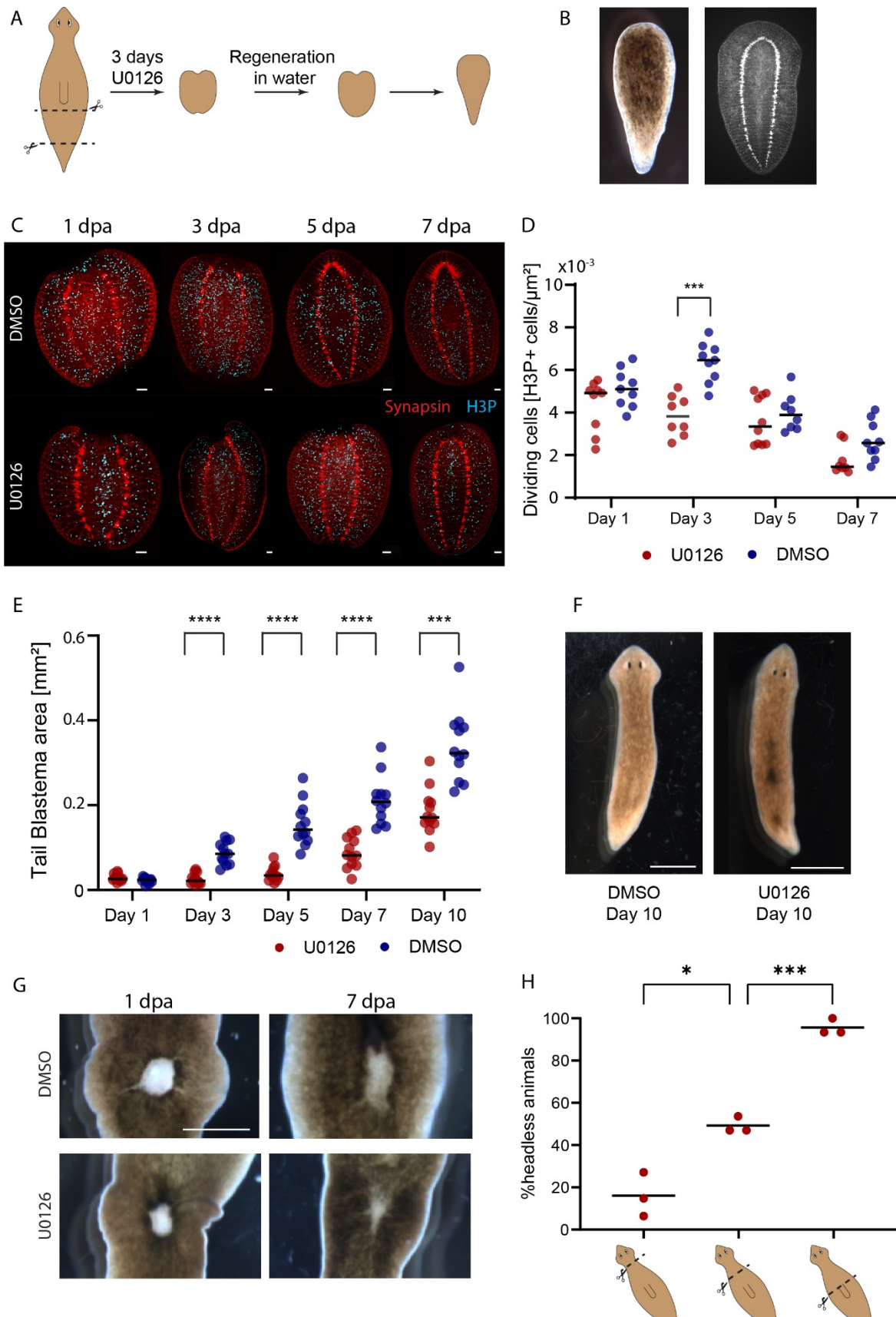
89 The regeneration of the nervous system under ERK inhibition has not previously been described  
90 in detail. Therefore, we used staining for synapsin to show the formation of the neural anatomy of the  
91 headless planarians. This staining revealed that instead of the clusters of neural tissue that are visible at  
92 Day 3 in control animals' anterior blastema, no staining indicative of brain formation was observed in  
93 U0126-treated samples. By Day 7 the two VNCs in the U0126-treated samples joined and form a rounded  
94 terminal structure (Figure 1C). These structures appeared to not form in the very small anterior blastema  
95 but rather in the underlying preexisting tissue.

96 ERK is known to play a crucial role in regulating cell division and we hypothesized that the lack of  
97 observed regeneration is due to a block of cell division. By staining for the cell division marker  
98 phosphohistone H3 (H3P), we observed that U0126-treated animals had significantly lower numbers of  
99 dividing cells at Day 3 compared to controls (Figure 1C, D), indicating a lack of the typical upregulation of  
100 cell division important in regeneration<sup>18</sup>. At the same time, there were still plentiful dividing cells even  
101 following 3 days of treatment with the highest tolerated dose of U0126.

102 The fact that dividing cells are observed even under the applied ERK inhibition may explain why,  
103 in addition to the clear lack of head regeneration, we found that the posterior wound of the fragments  
104 treated with U0126 formed a blastema and regenerated a normal tail shape (Figure 1B). To further  
105 investigate this apparent tissue-specific impact of ERK inhibition, we bisected animals and tracked tail  
106 regeneration on the anterior fragments following the 3-day treatment with U0126 (Figure 1E and F). The

107 blastema area was significantly smaller in ERK inhibitor treated animals compared to DMSO treated  
108 controls from Day 3 to Day 10 (Figure 1E). But even though regeneration was reduced in U0126-treated  
109 animals, a clear increase in size of the tail blastema over time was apparent in the treated animals (Figure  
110 1E) and the final regenerative outcomes at Day 10 were morphologically comparable to controls (Figure  
111 1F). Similarly, animals treated with the ERK inhibitor for 3 days were able to replace sections of internal  
112 tissue lost through a puncture (Figure 1G). This indicates that while temporary ERK inhibition reduces cell  
113 division and delays regeneration, this regenerative delay can be overcome and normal regeneration can  
114 be resumed for the formation of all tissues except the head, which is unable to recover from the  
115 temporary block. This differential response in regeneration of different structures suggests a separate  
116 head-specific role of ERK signaling in addition to its established role in regulating cell division. This  
117 observation is consistent with the reports that while ERK is active in both wound sites immediately after  
118 amputation, it remains persistently active for 72h only in the anterior blastema<sup>19</sup>.

119 The ERK inhibition we used to induce the headless phenotype was achieved via a pharmacological  
120 agent, U0126, which offers the opportunity of washing out the inhibitor and therefore lift the inhibition.  
121 To test the time frame in which the inhibitor is removed from the tissue following our washout at 3 dpa,  
122 we first performed a mass spectroscopy analysis on planarian tissues incubated in U0126 for 3 days 1 day  
123 after washout and 7 days after washout. 1 day after the tissue was removed from the U0126 solution,  
124 only trace amounts of the inhibitor were detected (Supplemental Figure 1A). To confirm that those trace  
125 amounts were below the threshold at which they were affecting regeneration, worm fragments were  
126 placed in U0126 for 3 days, washed out and placed in regular worm water for 1 day before being re-  
127 amputated and allowed to regenerate (Supplemental Figure 1B). 92% of re-amputated animals  
128 regenerated as single-headed animals (n=45), indicating that the amount of U0126 remaining in the tissue  
129 at Day 3 was below the concentration necessary to inhibit head regeneration (Supplemental Figure 1B).  
130 These results indicate that following the washout after the 3 day incubation with U0126, the inhibition of  
131 ERK activity is lifted rapidly and suggests that the head-regeneration specific role of ERK signaling is  
132 required in the early regeneration time window of the first 72 hours post amputation, known to be critical  
133 for polarity setting<sup>20,21</sup>, and cannot be later replaced within the original regeneration time window  
134 without further injury to trigger the response.



136 **Figure 1: ERK inhibition blocks regeneration in a tissue- and location-specific manner.** A) Experimental  
137 scheme showing the amputation planes of the pre-tail fragment treated with the ERK inhibitor U0126 for  
138 3 days before completing regeneration in water. B) ERK inhibition in pre-tail fragments leads to the  
139 formation of headless animals, shown in both outside morphology and underlying neural structure via  
140 synapsin staining. C) Staining for synapsin (red) and dividing cells (H3P - cyan) in fragments treated with  
141 U0126 or DMSO as control, fixed at 1, 3, 5 and 7 dpa (days post amputation). Scale bar 100  $\mu\text{m}$ . D)  
142 Quantification of the number of H3P foci/ $\mu\text{m}^2$  showing significant reduction of dividing cells in U0126  
143 treated samples (red) compared to control samples (blue) at Day 3. N=10 E) Size of the tail blastema  
144 following amputation and treatment with U0126 or DMSO, showing significant difference at all timepoints  
145 after 3 dpa. N=12 F) Representative image of animals at 10 dpa after U0126 and control treatment,  
146 showing morphologically similar tail regeneration. Scale bar 500  $\mu\text{m}$ . G) Progress of internal tissue  
147 regeneration following puncture wound at 1 dpa and 7 dpa in control and U0126 treated animals, showing  
148 similar progress of regeneration. Scale bar 500  $\mu\text{m}$ . H) Percentage of headless animals formed following  
149 amputation at different planes along the anterior-posterior axis and U0126 treatment, showing significant  
150 differences between the amputation planes. Remaining worms regenerated as single-headed animals.  
151 N=3x15. \*p< 0.05, \*\*\* p< 0.001, \*\*\*\* p<0.0001

152

153 *ERK inhibition blocks head formation in a location-specific manner*

154 The different response of anterior and posterior blastemas to ERK inhibition led us to ask whether  
155 additional positional effects were present in the response to ERK inhibition. We therefore decapitated  
156 animal at different planes, ranging from directly behind the auricles in the head to above the pharynx,  
157 before treating the decapitated fragments with U0126 for 3 days and observing the regenerative  
158 outcomes (Figure 1H). Surprisingly, we found that decapitations just below the head results in normal  
159 regeneration following U0126 treatment in the vast majority of cases, while decapitation at the top of the  
160 pharynx resulted in almost entirely headless regeneration (Figure 1H). The intermediate cutting plane led  
161 to a mixed regenerative outcome with 51 $\pm$ 4% single-headed animals while the remaining animals were  
162 headless (Figure 1H). Control animals regenerated as single-headed animals independent of cutting  
163 planes. This difference in regenerative outcomes is striking, as even the most anterior cutting plane  
164 requires reformation of the head with all its complex structures. The observed difference in regenerative  
165 ability along the A/P axis is reminiscent of the regeneration outcomes in animals treated with RNAi against  
166 the activin inhibitor Follistatin, which similarly showed headless regeneration only in more posterior

167 cutting planes<sup>11</sup>. This parallel conforms with previous reports that suggests that ERK ERK activity is  
168 upstream of follistatin<sup>7</sup> and indicates that ERK signaling may impact cell proliferation and differentiation  
169 differently in the context of a high Wnt signaling environment in the posterior compared to low Wnt  
170 anterior tissues. These connections between ERK and Wnt signaling are interesting in the light of studies  
171 showing interactions between these two signaling pathways in other systems<sup>22</sup> and the hypothesis that  
172 ERK and Wnt/β-catenin form opposing gradients starting from head and tail respectively in planarians<sup>9</sup>.

173 *Some headless animals repattern to normal morphologies over long time*

174 The headless animals that regenerate after ERK inhibition had previously been assumed to have  
175 reached a terminal, stable morphology<sup>7</sup>. We asked whether these animals would maintain their new  
176 morphology despite cell turnover or whether they would eventually be able to repattern to recover their  
177 original morphology (Figure 2A). Monitoring the headless animals for 18 weeks, we observed a remarkable  
178 phenotype in which some of the headless animals began to repattern, with some regaining a wild-type  
179 single-headed morphology. To quantify this phenomenon, we defined repatterning as any morphology  
180 change occurring after 4 weeks post-cutting. In headless animals observed from when they were cut until  
181 their death (n=181), 22% showed some form of repatterning (Figure 2B). Importantly, this repatterning  
182 occurred without any intervention. To ensure that no wounding happened to induce regeneration,  
183 animals were kept separated in individual wells and were not handled. No injury was observed during the  
184 weekly microscopic inspection of the animals. The remaining 78% of headless animals did not show any  
185 change in morphology except for shrinking in size, as headless animals are unable to feed and therefore  
186 have a limited lifetime. We observed repatterning from 4 weeks onwards with the majority of repatterning  
187 occurred between 4 and 10 weeks (Figure 2C). After 10 weeks only sporadic new repatterning was  
188 observed, although some worms began forming new heads as late as 18 weeks after cutting. This  
189 spontaneous repatterning that allows the re-establishment of a normal morphology many weeks after  
190 regeneration is completed suggests the existence of tissue processes that operate on a time scale much  
191 longer than previously known which trigger the re-emergence of normal body parts. The fact that we  
192 observe this repatterning, contrary to previous reports that suggested ERK-induced headlessness is a  
193 stable morphology, is most likely due to the longer timeframe of observation. Owlarn et al. state that  
194 headless animal remained headless even 18 days after amputation<sup>7</sup>, which does not contradicting our  
195 observation of repatterning 30+ days following amputation. Previous investigations of headless animals  
196 also mainly used the *Schmidtea mediterranea* species while we use *Dugesia japonica*, and the onset of  
197 repatterning may be distinct in the two species.

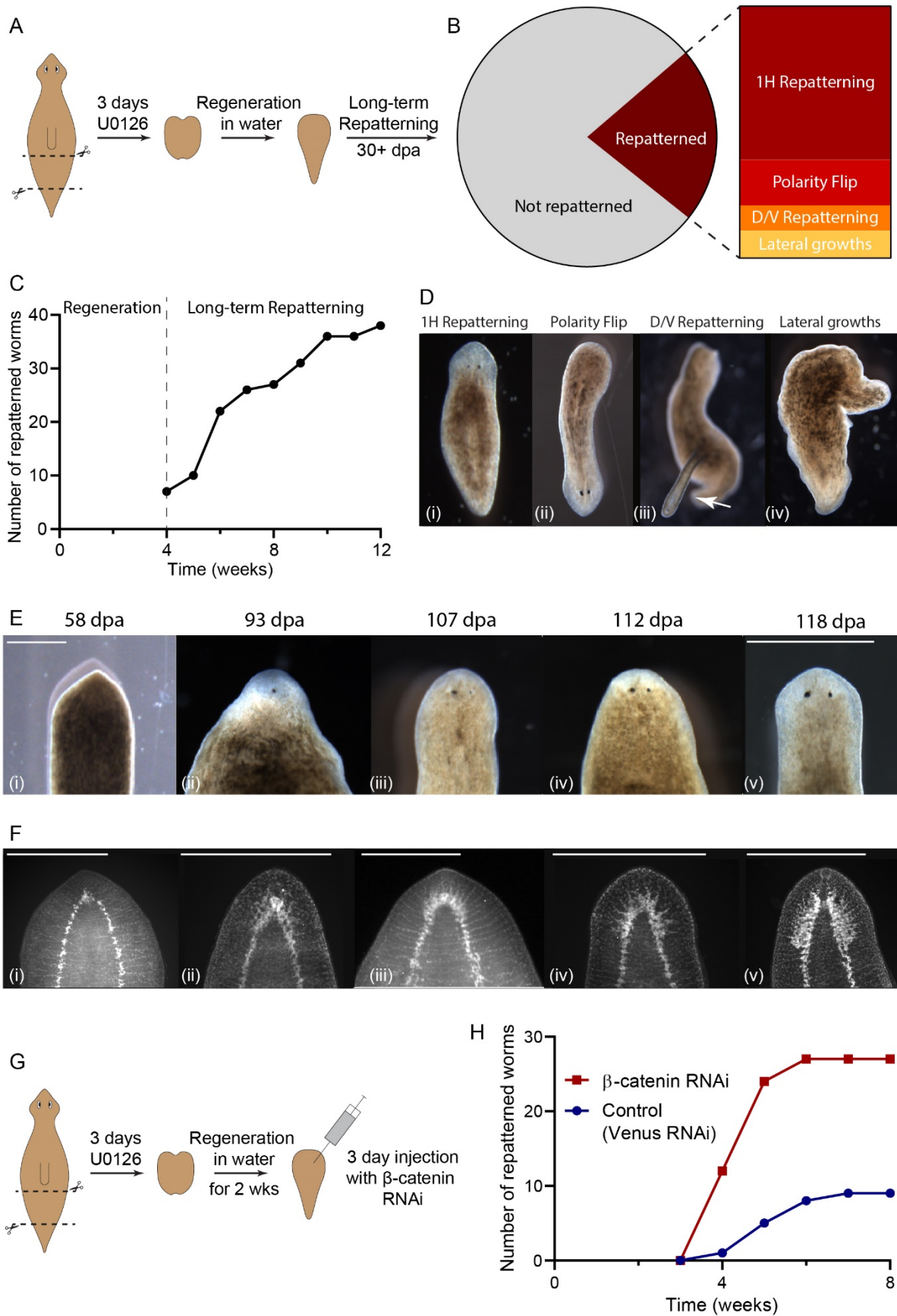
198 Anatomically, the observed repatterning fell into 4 different categories. The most common  
199 repatterning type was single-headed repatterning where a normal wild-type morphology was regained  
200 (61% of all repatterning worms, Figure 2B, Di). Strikingly, the second most common phenotype was a  
201 polarity reversal, in which, following fissioning of a headless animal, the posterior blastema formed into a  
202 head (18%, Figure 2B, Dii). The remaining two categories represent the rare animals that exhibited  
203 growths which did not lead to the formation of a head, either in the form of dorsal outgrowths (D/V  
204 repatterning, 10%, Figure 2Diii) or lateral outgrowths (11%, Figure 2Div).

205 When headless animals repatterned to form a new head, the pigmentation of the round anterior  
206 end began to lighten and the tissue flattened out, forming a structure resembling a blastema (Figure 2E).  
207 Once this “blastema” formed, first one eyespot appeared (Figure 2E ii) and then the second one formed  
208 with a few days delay (Figure 2E iii), along with the head reshaping to regain the typical triangular  
209 morphology (Figure 2E iv and v). Animals were stained using synapsin antibodies to visualize the regrowth  
210 of the underlying brain tissue at intervals during the repatterning process. This showed that early brain  
211 repatterning occurred via the formation of a cluster of neural tissue at the anterior rounding of the VNC  
212 (Figure 2F i). Brain structures formed progressively from there, first in an apparently unorganized manner  
213 (Figure 2F ii), before expanding and reforming into a well-organized brain resembling that of a normal  
214 animal (Figure 2F iii-v). While the repatterning process resembles normal head regeneration in its  
215 progression, the timeframe was distinctly slower than normal head regeneration<sup>23</sup>, taking up to 25 days  
216 from the first observation of changes at the anterior to a fully formed head.

217 The observation that planarians are capable of recovering a wild-type bodyplan by spontaneously  
218 triggering a regeneration-like process, after maintaining a stable abnormal morphology for long periods  
219 of time, poses interesting questions about how abnormal morphologies are first maintained and how they  
220 are eventually detected to trigger correction. In other organisms there is some evidence that remodeling  
221 of tissues to fit new morphologies can be part of regeneration, such as the remodeling of transplanted tail  
222 tissue into a limb in amphibia<sup>24</sup>. The repatterning reported here is distinct from previous studies where  
223 it was shown that general injury signals can induce regeneration in headless animals<sup>7</sup>, as here there is no  
224 triggering injury of any kind. The here demonstrated ability to mount a regenerative response without  
225 any injury to trigger it is consistent with the idea that a missing tissue response (MTR) may not be  
226 necessary for regeneration to occur<sup>11</sup>. Our finding that the spontaneous repatterning is slower than  
227 normal regeneration is also consistent with other examples of regeneration in the absence of the MTR<sup>11</sup>.

228        The timepoint at which repatterning starts appears to be stochastic within the population. We  
229        showed that size was not a trigger for repatterning, as fragments of very different sizes could start  
230        repatterning at similar times (Supplemental Figure 2). This lack of correlation between repatterning size  
231        and timing rules out the starvation-induced shrinking as a trigger for repatterning.

232        Given that Wnt/β-catenin signaling is crucial in regulating head regeneration in planarians<sup>25</sup>, we  
233        investigated whether blocking Wnt signaling is able to drive repatterning in headless worms by injecting  
234        headless planaria with β-catenin dsRNAi and tracking their repatterning rates compared to headless  
235        animals injected with control dsRNAi (Figure 2G). Even though injection causes minor injury, we chose this  
236        method of dsRNAi administration due to the fact that headless planaria are unable to feed to ingest  
237        dsRNAi. We controlled for the injection-induced injury by the injection of a control dsRNAi, which led to a  
238        repatterning rate very similar to non-injected headless animals. In β-catenin RNAi animals, we saw  
239        repatterning of 100% of headless animals by 6 weeks after initial amputation, which was significantly more  
240        than in control RNAi-injected animals, where only around 30% repatterned in the same timeframe (Figure  
241        2H). This suggests that repatterning uses the same signaling pathways that regulate normal head  
242        regeneration and that the start of repatterning may be dependent on Wnt signaling activity.



244 **Figure 2: Headless animals can regain normal morphology over long timeframes.** A) Illustration of the  
245 experimental procedure in which pre-tail fragments were treated for 3 days with U0126 to induce  
246 headless animals which were then observed for changes in morphology over long timeframes. B) Out of  
247 181 headless worms tracked individual over time, 22% repatterned, while the remaining 78% did not  
248 change their morphology. The repatterned animals fell into 4 different categories – 61% Single-head (1H)  
249 repatterning, 18% polarity flip, 10% D/V repatterning, and 11% Lateral growths. C) Repatterning rate over  
250 time showing steady increase in the number of repatterned animals from 4 to 10 weeks after the initial  
251 amputation. D) Representative images of the 4 different repatterning types – i) 1H repatterning, ii) Polarity  
252 flip, iii) D/V repatterning (arrow marking dorsal outgrowth), and iv) Lateral growths. E) Repatterning to  
253 regain a single-headed morphology in one animal tracked over time. Scale bar 500  $\mu$ m. F) Samples fixed  
254 and stained with synapsin antibody at different stages of repatterning, arranged into a putative neural  
255 repatterning timeline. Scale bar 500  $\mu$ m. G) Experimental procedure with injection of  $\beta$ -catenin dsRNA or  
256 control dsRNA on 3 consecutive days into headless animals 14 days after initial induction. H) Repatterning  
257 rate in  $\beta$ -catenin RNAi (red) compared to Venus RNAi (blue) control animals. N=2x15.

258

259 *Headless worms can reverse polarity following posterior injury*

260 One of the unexpected repatterning phenotypes we observed was a polarity reversal, which  
261 occurred following spontaneous fissioning of headless animals. We observed fissioning even in headless  
262 animals that had not fed for a long time, showing that in *Dugesia japonica* fissioning can take place in the  
263 absence of a head and under low nutrition conditions. Following fissioning, the tail fragment always  
264 regenerated as a single-headed animal, as here the fissioning wound recapitulates an injury inducing head  
265 formation (Supplemental Figure 1). However, the anterior fragment has a more interesting, stochastic  
266 fate. In 85% of cases (82/96 observed fissioned animals), the anterior fissioning fragment regenerated the  
267 lost tail and remained headless. However, in the remaining 15% of cases (n=14/96) the anterior fissioning  
268 fragment underwent regeneration in which the posterior blastema formed into a head rather than a tail  
269 (Figure 3A). This resulted in the formation of single-headed animals with a head on the previously  
270 posterior end. In those animals, the rounded, formerly anterior, end repatterned into a typical pointed  
271 tail shape (Figure 3A iii-v). The single-headed animals arising from this polarity reversal exhibited striking  
272 movement patterns, in which the tail led the direction of the movement as opposed to the head in normal  
273 animals (Supplemental Movie 1). This abnormal movement confirms the reversal of polarity and is in line  
274 with the observed slow adaptation of cilia orientation in newly formed double-headed animals to their

275 new morphology<sup>26</sup>. A spontaneous polarity reversal has not been reported in planaria, although  
276 previously worked induced head growth at the posterior blastema through application of electrical  
277 currents<sup>27</sup>.

278 This fascinating observation of a reversal of polarity following fissioning led us to investigate  
279 whether this reversal of polarity could also be induced by a posterior cut in headless animals. We  
280 therefore bisected headless animals at 4 weeks after induction at various planes along the A/P axis and  
281 observed the regenerative outcomes in the anterior fragments of all these cuts. Polarity reversal occurred  
282 in fragments from all different cutting planes, although at highly variable rates between experiments  
283 independent of the cut position (Supplemental Figure 3).

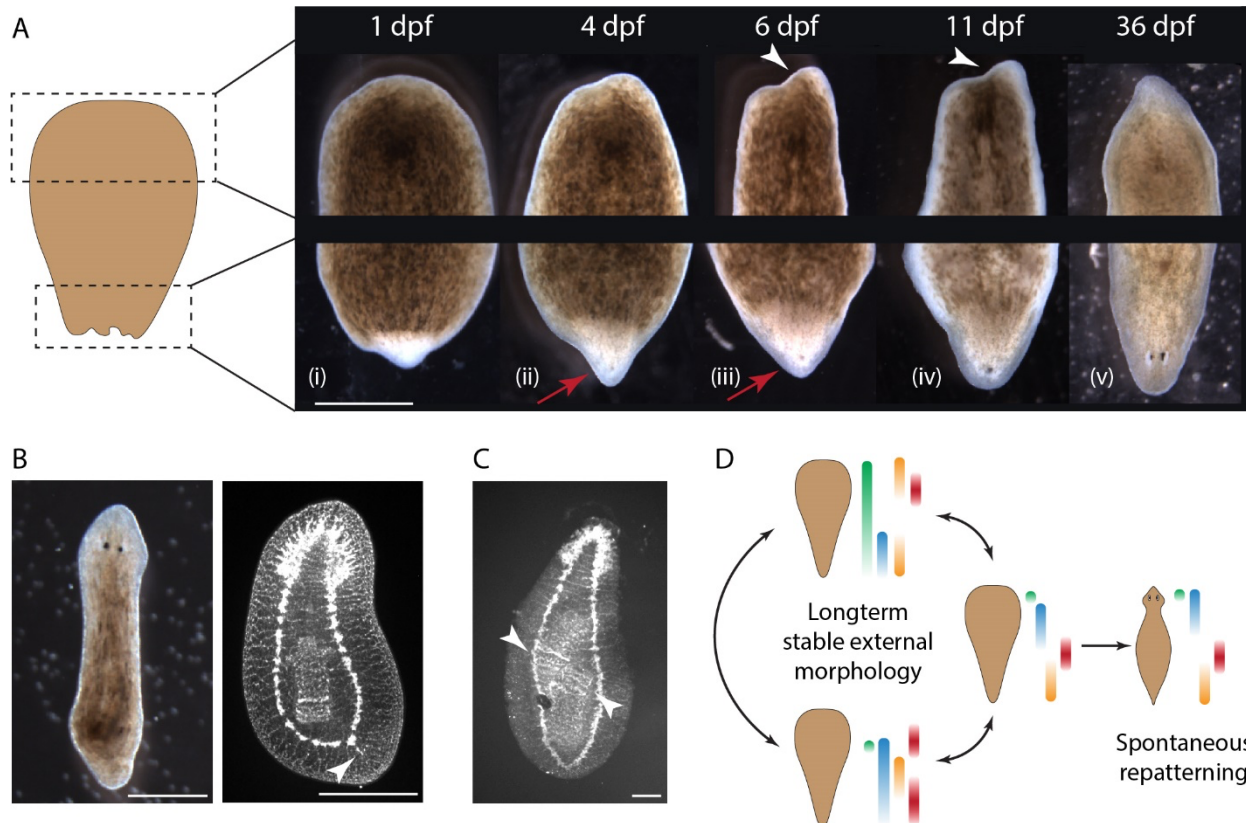
284 In animals that reversed their polarity, the nervous system regeneration went along with external  
285 morphology, with a normal brain forming in the posterior blastema (Figure 3B). At the same time, the  
286 formerly rounded VNC terminus began to branch out to reform the more pointed VNC tail morphology  
287 (Figure 3B). This however happened with a delay compared to the outward morphology, as worms with a  
288 relatively normal outward tail morphology were observed with the underlying nervous system only  
289 beginning to branch out (Figure 3B). Other internal structures also adjust to the new organismal polarity,  
290 often leading to abnormal intermediate states, such as worms with two pharynxes with opposing  
291 orientations (Figure 3C).

292 At the same time, many headless animals showed abnormal pharynx placement and orientation  
293 even before repatterning (Supplemental Figure 4). Most headless animals possessed pharynges at the  
294 very anterior end, directly abutting the rounded VNC anterior (Supplemental Figure 4A). At the same time,  
295 headless animals existed with multiple pharynges, either oriented perpendicular to each other and to the  
296 body axis (Supplemental Figure 3B) or aligned with the body axis but in opposing orientations to each  
297 other (Supplemental Figure 3C). The presence of animals with multiple and mispositioned pharynges may  
298 be indicative of a generally disturbed underlying whole-body axial polarity in headless animals, which  
299 results in a failure of signals about number and orientation of organ-level structures, leading to the  
300 disrupted formation of the pharynxes in location and orientation<sup>28</sup>.

301 Combining the observation of the polarity reversal at posterior injuries independent of A/P  
302 position with the identification of misplaced pharynges suggests a hypothesis explaining headless  
303 repatterning (Figure 3D). Headless animals may exhibit disorganized expression of the position control  
304 genes (PCGs) which control both regenerative outcomes and tissue maintenance<sup>29</sup>. Such a disorganized

305 expression of regulating factors would explain why in a limited number of cases a posterior blastema gives  
306 rise to a head and why pharynges are formed in incorrect locations and positions. If the expression  
307 domains of the PCGs are not only mispositioned but also dynamically changing, this would explain the  
308 spontaneous starting times of repatterning of headless animals as resulting from the random alignment  
309 of a sufficient number of signaling factors to trigger tissue growth and formation of correct structures.

310



311

312 **Figure 3: Headless worms can reverse their polarity.** A) In the anterior fissioning fragment of a headless  
313 animal, the posterior blastema regenerates into a head, including the formation of an eyespot at 4 days  
314 after fissioning (red arrows). At the same time, the rounded anterior changes its morphology to a more  
315 typical tail-like morphology (white arrowheads). B) A single-headed worm resulting from polarity reversal  
316 in brightfield and synapsin staining of the same animal, illustrating normal brain morphology formed in  
317 the posterior blastema and beginning of changes in the VNC structure in the new tail (white arrowhead).  
318 Scale bar 500 µm C) Synapsin staining of a single-headed animal arising from polarity reversal with two  
319 pharynges, the upper in the correct head-tail orientation and the lower in the opposite orientation, as  
320 visible by the distinct band and denser innervation around the pharynx mouth (white arrow). Scale bar

321 100 µm. D) Scheme illustrating the hypothesized misexpression of PCG domains that drives spontaneous  
322 repatterning of headless animals and polarity reversal.

323

324 **Conclusion**

325 ERK signaling is crucial in regulating the cell division required for regeneration. We show here that in  
326 planarian flatworms, ERK inhibition during the first 3 days of regeneration can be overcome in all tissues,  
327 except in regeneration of the head, suggesting a secondary signaling function for ERK in head formation.  
328 In the context of head regeneration, we present data that suggests that ERK signaling interacts with other  
329 signaling pathways, as ERK inhibition only blocks head regeneration in the posterior tissues which have  
330 high Wnt signaling activity, arguing for an interaction of ERK and Wnt signaling in regulating head  
331 regeneration.

332 We further report the surprising finding that the headless animals that form following ERK inhibition do  
333 not remain permanently headless, but over very long timeframes spontaneously begin to repattern and  
334 regain their normal morphology. In some of the headless animals, repatterning goes along with reversal  
335 of prior anterior-posterior axial polarity, suggesting an underlying instability of pattern signaling. The very  
336 long timeframe of the repatterning process (up to 18 weeks) poses interesting questions about what  
337 factors or physiological processes can be responsible for sensing mispatterning or triggering remodeling  
338 in this timeframe. It also suggests that other planarian regeneration outcomes should be observed over  
339 much longer times than is currently practiced, as other fascinating long-term effects may be discovered  
340 through this.

341 **Methods**

342 *Colony maintenance*

343 *Dugesia japonica* were maintained in Poland Spring water at 20°C, fed calf liver paste once a week  
344 and cleaned twice a week, as described in <sup>30</sup>. Animals were starved for one week prior to usage in  
345 amputation and pharmacological treatment experiments and were not fed for the duration of all  
346 experiments.

347 *Animal manipulation*

348 Cutting of planaria was performed on a cooling plate using scalpel fragments. For generating  
349 headless animals, pre-tail fragments were cut by placing a cut at the pharynx opening and another cut  
350 narrowly above the tail tip. For tracking tail regeneration, animals were cut halfway between the head  
351 and tail. For tracking regeneration along the A/P axis, animals were either decapitated narrowly by cutting  
352 just below the auricles, cut halfway between the base of the head and the top of the pharynx, or cut  
353 directly at the top of the pharynx. To track regeneration of internal tissue a puncture wound was induced  
354 using square glass capillaries of a 0.7 mm<sup>2</sup> inner diameter (VitroCom, Mountain Lakes, NJ) directly  
355 posterior to the pharynx opening. A fine paintbrush was used to remove the cut tissue from the middle of  
356 the animal.

357 *Pharmacological Treatments*

358 Headless worms were produced through transient pharmacological treatment of freshly cut pre-  
359 tail fragments in 18 μM U0126 dissolved in DMSO (Sigma). No more than 40 fragments were treated per  
360 10 cm petri dish. Fragments were incubated in U0126 for 3 days at 20°C before washing out the drug  
361 solution. At 14 days post amputation, the fragments were scored for regenerative phenotype.

362 *Scoring of Repatterned Phenotypes*

363 Headless animals were maintained in individual wells of 12-well plates and their phenotypes were  
364 scored weekly for the duration of the experiment. Any significant changes in morphology, such as head  
365 regeneration, fissioning, or ectopic tissue development were noted. Time of repatterning was determined  
366 once one eye was visible in the forming head structure. Worms were labelled as “Polarity Flip” when a  
367 headless worm fissoned and a head regenerated at the posterior wound site. Worms were labelled as  
368 “Dorsal/Ventral repatterning” when an outgrowth of tissue occurred in the D/V plane of the headless

369 worm. Worms were labelled as “Lateral growth” when significant changes in morphology occurred with  
370 growth on the lateral area of the animal, resulting in stable morphology which did not produce a head.

371 *RNA Interference*

372 For  $\beta$ -catenin RNAi treatments, headless animals were selected at 14 dpa and injected on 3  
373 consecutive days with dsRNA for *D. japonica*  $\beta$ -catenin and control dsRNA for VenusGFP. dsRNA was  
374 generated and injected as noted in <sup>31</sup>. 3 pulses of RNAi/per worm were given each day for 3 consecutive  
375 days.

376 *Mass Spectroscopy analysis of U0126 levels*

377 Samples for MassSpec were generated by collecting fragments either directly from U0126  
378 solution or following washout, removing all water, and placing 3 mm glass beads (Milipore, Burlington,  
379 MA) into an Eppendorf tube. Tissue was disrupted by vortexing for 2 min. DMSO was added as a solvent  
380 to the disrupted tissue and samples were vortexed again for 1 min. Liquid was removed from the beads  
381 and centrifuged for 20 min at 14,000 rotations per minute at 4°C. The upper clear phase was removed and  
382 filtered through a 0.2  $\mu$ m polytetrafluoroethylene-syringe filter (Whatman, Maidstone, UK). Samples were  
383 stored at -80°C before analysis. U0126 standard was prepared by diluting in DMSO.

384 The samples were analyzed by the Harvard Faculty of Arts and Sciences Core Facility, on a Bruker  
385 Impact HD q-TOF mass spectrometer. Each LC-MS run was calibrated with known m/z values from sodium  
386 formate clusters. The LC column used was a henomenex Kinetex C18 (150 mm, 2.1 mm ID, 2.6  $\mu$ m particle  
387 size). The HPLC method used 0.1% formic acid as mobile phase A and 0.1% formic acid in acetonitrile as  
388 mobile phase B. 5% B was used for the first 2 minutes, while the eluent was diverted to waste using a  
389 divert valve. At 2 minutes, the eluent was sent to the mass spectrometer. The mobile phase composition  
390 was changed linearly from 5% B to 100% B over 10 minutes. The composition was returned to 5% B over  
391 0.1 minutes and kept constant for another 3.9 minutes to re-equilibrate the system to starting condition.  
392 A constant flow rate of 200  $\mu$ L/min and an injection volume of 5  $\mu$ L was used for all samples.

393

394 *Immunohistochemistry and Imaging*

395 Worms were fixed in Carnoy’s fixative (2% HCl treatment to remove mucous, followed by fixing  
396 solution composed of 60% Ethanol, 30% Chloroform, and 10% Glacial Acetic Acid) and stained using  
397 primary antibodies anti-synapsin (SYNORF-1) (Developmental Studies Hybridoma Bank (DSHB), University  
398 of Iowa) at 1:50 and anti-phosphorylated histone H3 (H3P) (Invitrogen) at 1:250 dilution. Anti-SYNORF1

399 was deposited to the DSHB by Buchner, E. (DSHB Hybridoma Product 3C11 (anti SYNORF1))<sup>32</sup>. Secondary  
400 antibodies used were goat-anti-mouse Alexa488 (Sigma, St. Louis, MO, USA) and a goat-anti-rabbit-  
401 Alexa555 (Sigma) at 1:400 dilution. Samples were mounted in Vectashield® hard set mounting medium  
402 (Vector Laboratories, Burlingame, CA) and imaged on a Nikon AZ100M stereoscope or a Leica SP8 confocal  
403 (Leica, Mannheim, Germany) with HyD detector, 488 and 552 nm diode light source, and 10x NA=0.4  
404 (Leica HC PL APO CS2) objective.

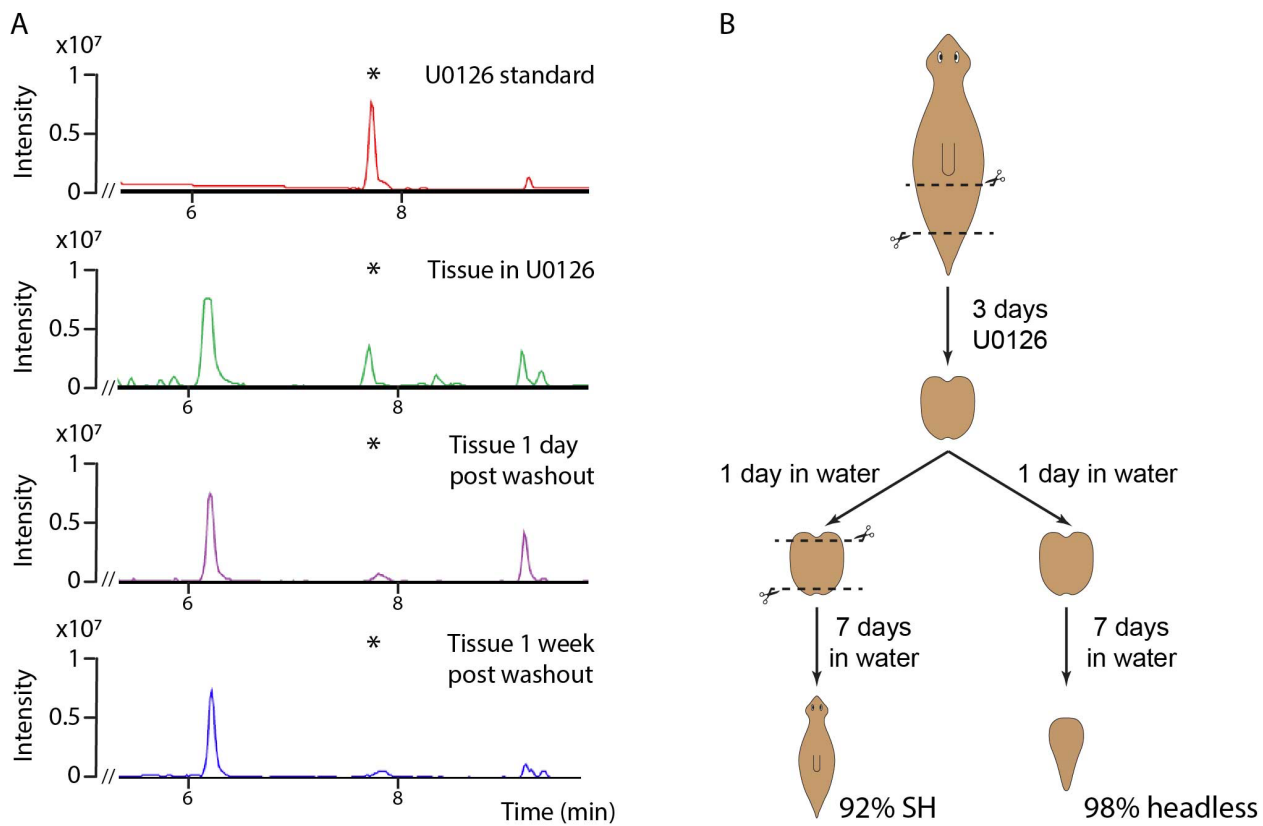
405 *Image and Data analysis*

406 All image analysis was performed in Fiji ImageJ<sup>33,34</sup>. To detect H3P positive cells, samples were  
407 thresholded using the Moments method, and the Analyze Particle function was used to count spot above  
408 a size of 10 pixels. All other analysis was performed manually. Data visualization and statistical analysis  
409 was performed in GraphPad Prism 8.2.1. ANOVA with Bonferroni post-correction were performed to  
410 determine significance.

411 *Data availability*

412 All raw data is available upon request.

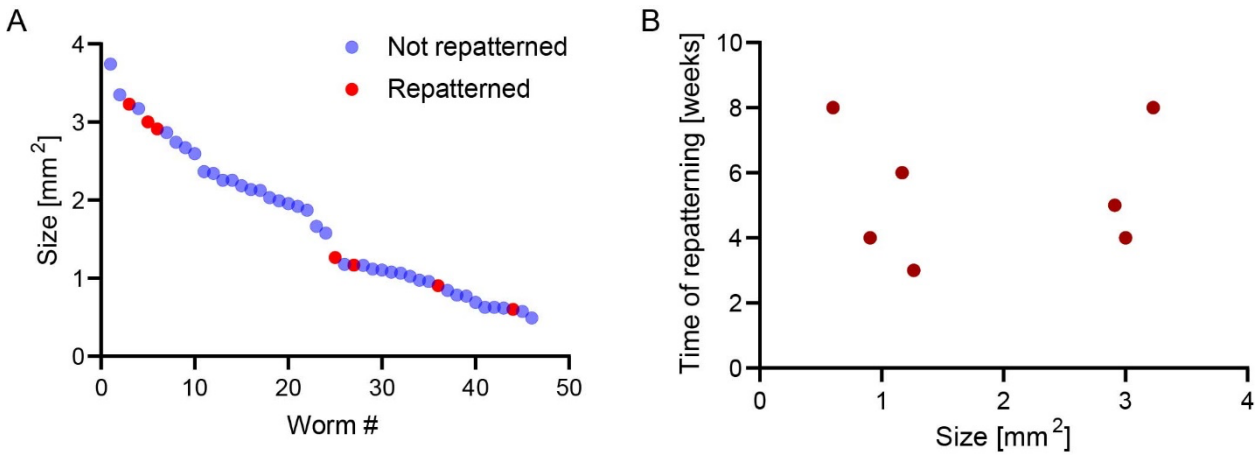
413 **Supplementary Materials**



414

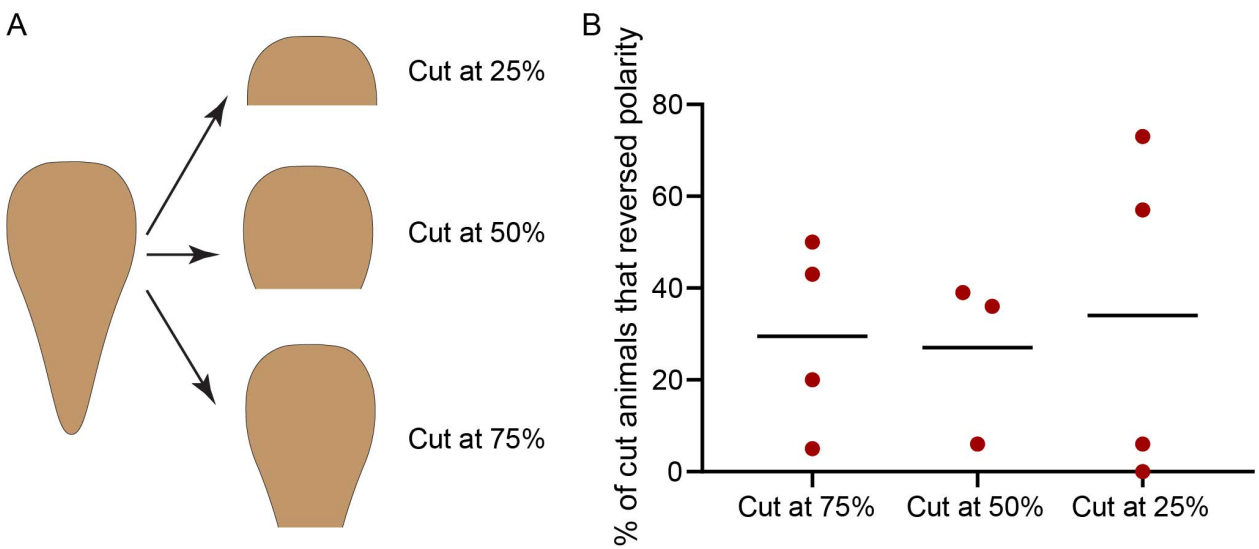
415 **Supplemental Figure 1: U0126 absence in tissue after washout.** A) Mass spectroscopy analysis of a U0126  
416 standard compared to extracts from planarian tissue incubated with U0126, tissue 1 day after washout  
417 from U0126 and 1 week after washout. Asterisk marks the characteristic U0126 peak. B) To show that the  
418 levels of U0126 remaining in the tissue 1 day after washout were not sufficient to inhibit regeneration,  
419 fragments were recut at 1 day after washout from U0126 before being allowed to regenerate. N=3 repeats  
420 of 15 animals each.

421



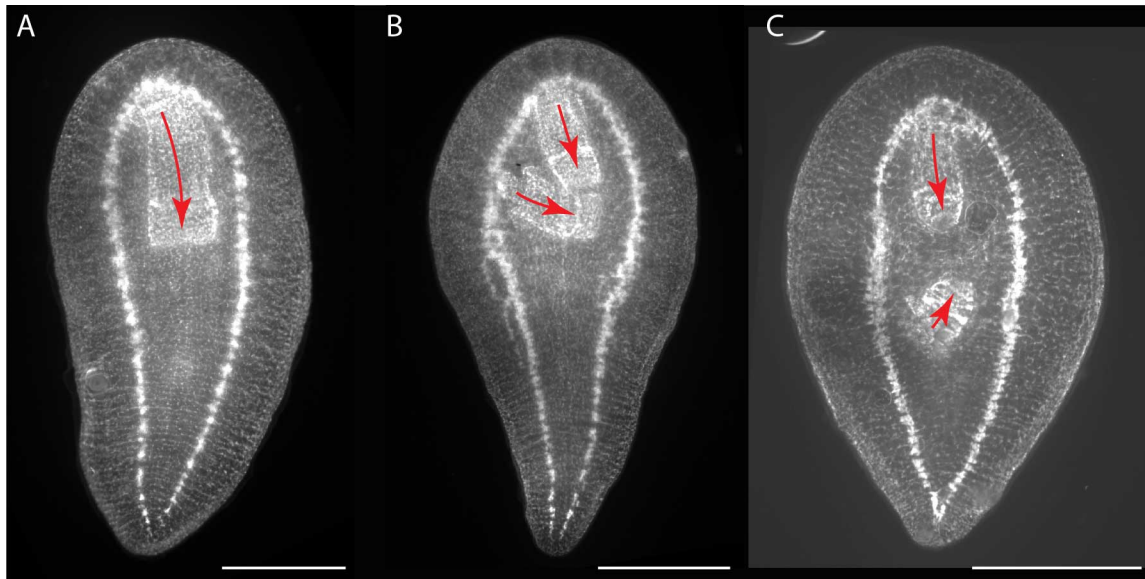
422

423 **Supplemental Figure 2: Timepoint of repatterning is independent of animal size.** A) Size of all animals  
424 followed in this experiment showing wide range of sizes. Red points mark any animal that repatterned  
425 within the 8-week experimental timeframe. B) Repatterning timepoint plotted against size of the  
426 repatterned animal at the start of the experiment.



427

428 **Supplemental Figure 3: Polarity reversal results from cutting at variable rates.** A) Experimental scheme  
429 showing the different planes at which the headless animals were cut. B) Percentage of animals that  
430 underwent polarity reversal following cuts at the respective planes. Each data point represents an  
431 independent repeat with 15 animals each.



432

433 **Supplemental Figure 4: Synapsin stain of headless animals illustrating different pharynx positions.** A)  
434 Headless animal with an anteriorly positioned pharynx. B) Headless animal with two pharynxes, one  
435 perpendicular to the head-tail axis. C) Headless animal with two pharynxes in opposing orientations. Scale  
436 bar 500  $\mu\text{m}$ . Arrows illustrate pharynx orientation.

437 **Supplementary Video 1: Single-headed animal resulting from polarity reversal freely moving.**

438

439 **Acknowledgements:**

440 The authors would like to thank Anna Kane, Joshua Finkelstein, and all members of the Levin lab  
441 for thoughtful discussions on this project. We thank Hans Gonzembach for planaria colony maintenance.  
442 This research was supported by the Allen Discovery Center program through The Paul G. Allen Frontiers  
443 Group (12171), and by the National Institutes of Health Research Infrastructure grant NIH S10 OD021624.  
444 We also gratefully acknowledge support of the Barton Family Foundation and the Elisabeth Giaque Trust.

445

446 **Author contribution:**

447 Conceptualization: JB, JVL, CF, ML

448 Methodology Development: JB, JVL

449 Validation: JB, KAM

450 Formal Analysis: JB

451 Investigation: JB, JVL, KAM, KBW, JM

452 Resources Provision: ML

453 Data Curation: JB

454 Writing – Original Draft: JB

455 Writing – Review & Editing: JB, JVL, KAM, KBW, JM, CF, ML

456 Visualization: JB, JVL

457 Supervision: JB, ML

458 Project Administration: JB, ML

459 Funding Acquisition: ML

460

461 **Competing Interest:**

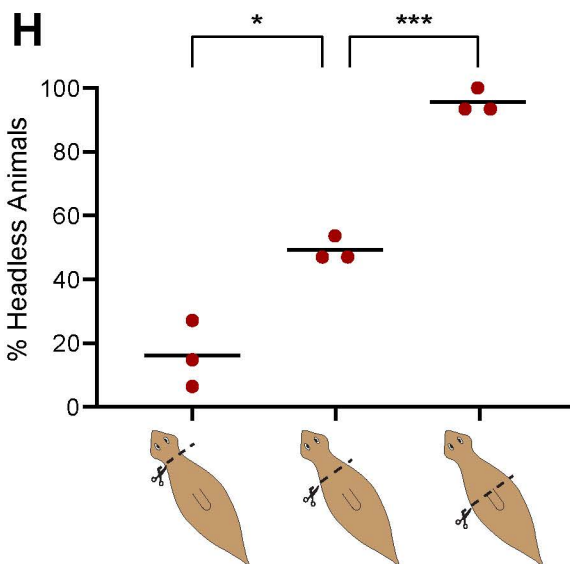
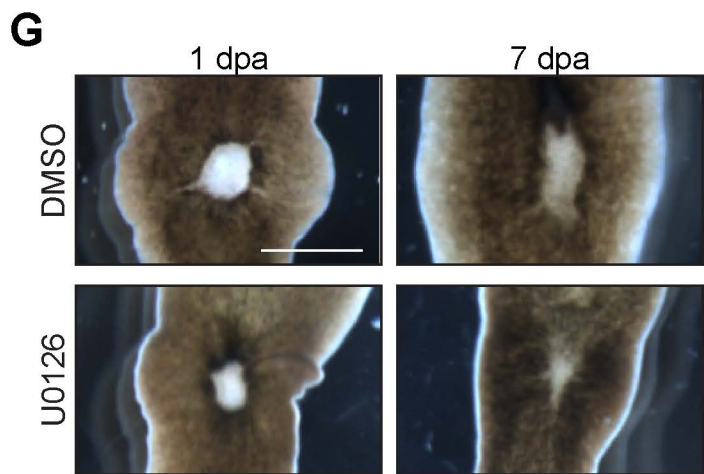
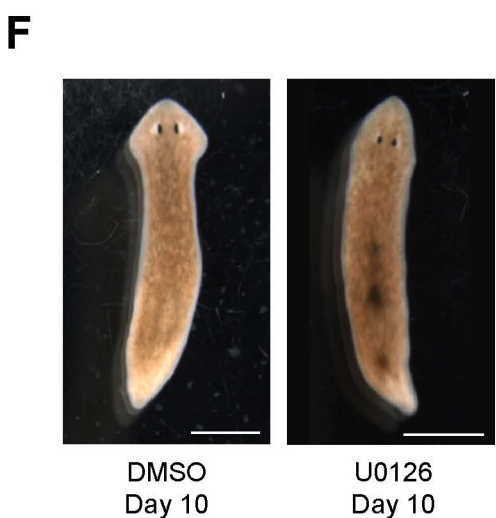
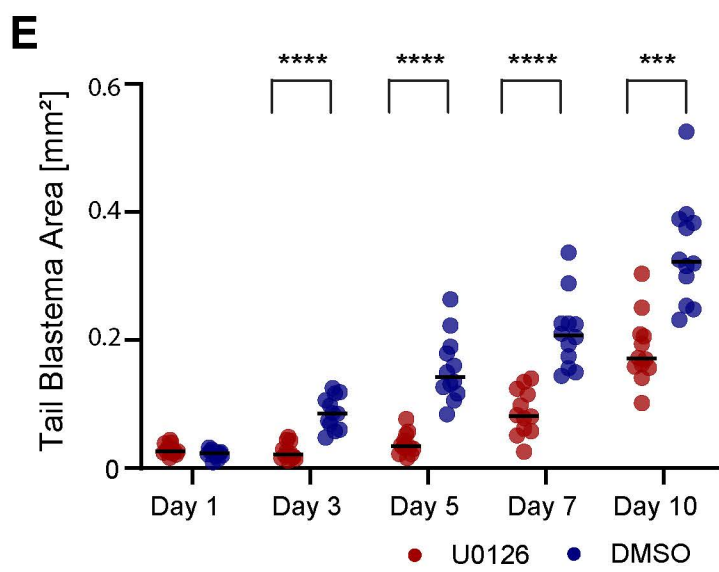
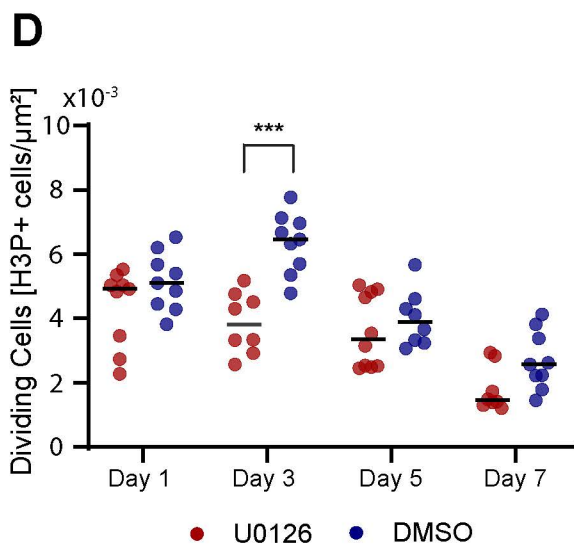
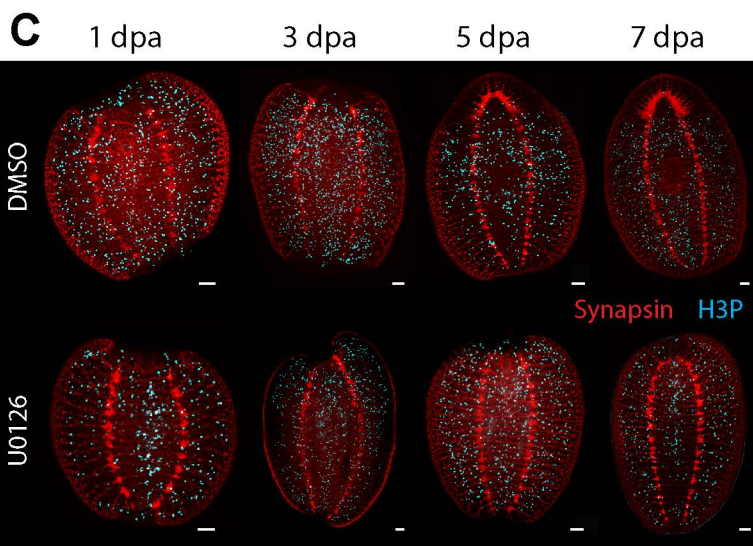
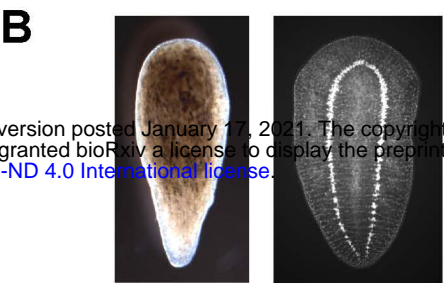
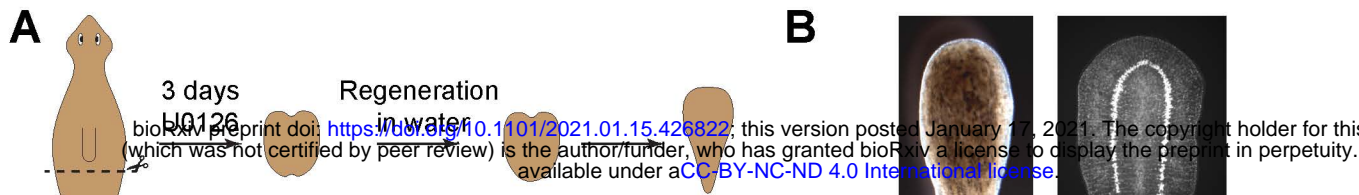
462 The authors declare no competing interests.

463 **References**

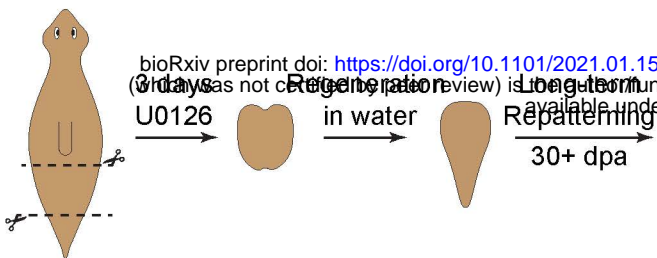
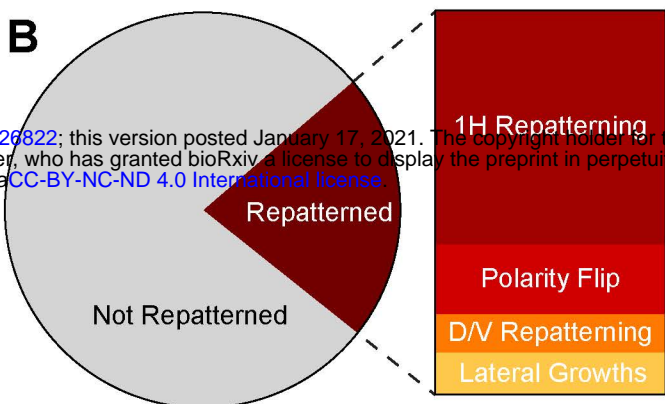
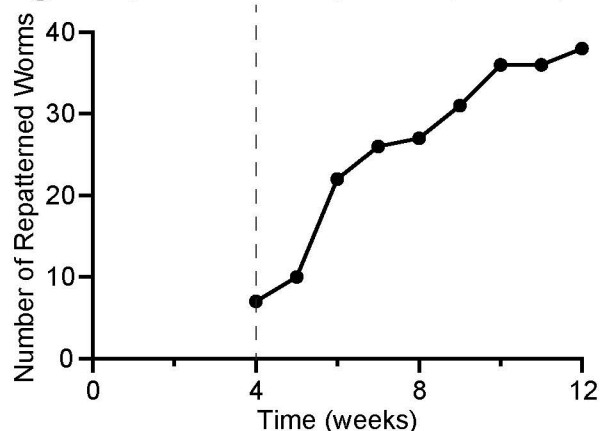
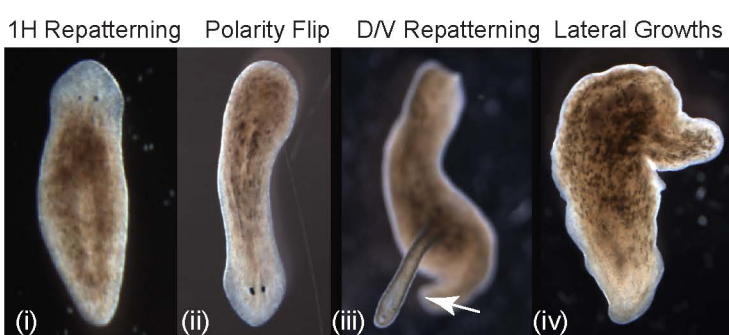
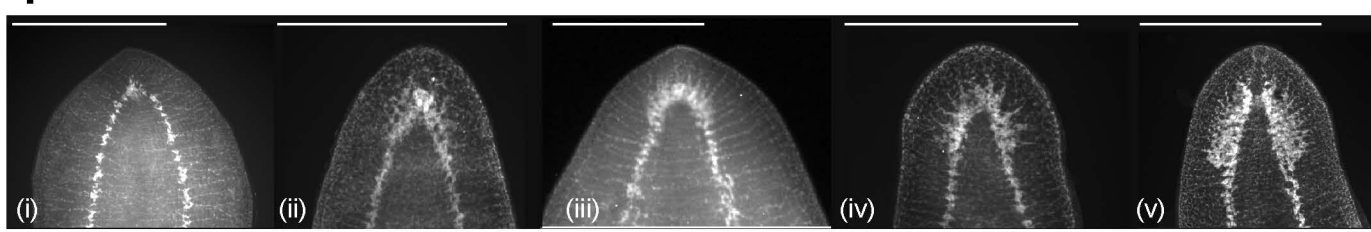
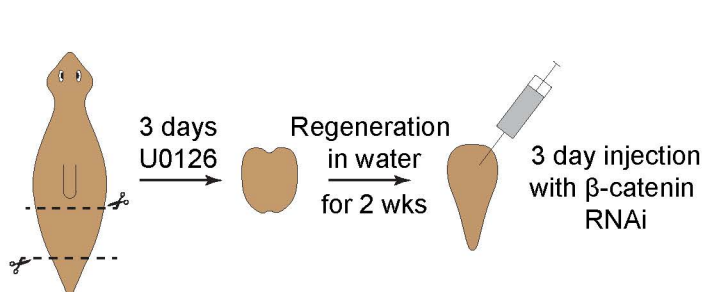
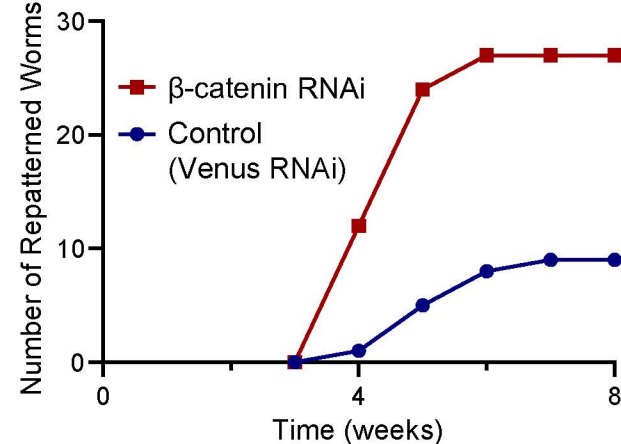
- 464 1. Birnbaum KD, Alvarado AS. Slicing across kingdoms: regeneration in plants and animals. *Cell*. Feb  
465 22 2008;132(4):697-710.
- 466 2. Tanaka EM, Reddien PW. The cellular basis for animal regeneration. *Dev Cell*. Jul 19  
467 2011;21(1):172-85. <https://doi.org/10.1016/j.devcel.2011.06.016>.
- 468 3. Gehrke AR, Srivastava M. Neoblasts and the evolution of whole-body regeneration. *Curr Opin  
469 Genet Dev*. Oct 2016;40:131-137. <https://doi.org/10.1016/j.gde.2016.07.009>.
- 470 4. Sun Y, Liu WZ, Liu T, Feng X, Yang N, Zhou HF. Signaling pathway of MAPK/ERK in cell  
471 proliferation, differentiation, migration, senescence and apoptosis. *J Recept Signal Transduct  
472 Res*. 2015;35(6):600-4. <https://doi.org/10.3109/10799893.2015.1030412>.
- 473 5. Yun MH, Gates PB, Brockes JP. Sustained ERK activation underlies reprogramming in  
474 regeneration-competent salamander cells and distinguishes them from their mammalian  
475 counterparts. *Stem Cell Reports*. Jul 8 2014;3(1):15-23.  
<https://doi.org/10.1016/j.stemcr.2014.05.009>.
- 477 6. Tasaki J, Shibata N, Nishimura O, et al. ERK signaling controls blastema cell differentiation during  
478 planarian regeneration. *Development*. Jun 2011;138(12):2417-27.  
<https://doi.org/10.1242/dev.060764>.
- 480 7. Owlarn S, Klenner F, Schmidt D, et al. Generic wound signals initiate regeneration in missing-  
481 tissue contexts. *Nat Commun*. Dec 22 2017;8(1):2282. [https://doi.org/10.1038/s41467-017-02338-x](https://doi.org/10.1038/s41467-017-<br/>482 02338-x).
- 483 8. Bohr TE, Shiroor DA, Adler CE. Planarian stem cells sense the identity of missing tissues to launch  
484 targeted regeneration. *bioRxiv*. 2020. <https://doi.org/10.1101/2020.05.05.077875>.
- 485 9. Umesono Y, Tasaki J, Nishimura Y, et al. The molecular logic for planarian regeneration along the  
486 anterior-posterior axis [Research Support, Non-U.S. Gov't]. *Nature*. Aug 1 2013;500(7460):73-6.  
<https://doi.org/10.1038/nature12359>.
- 488 10. Reddien PW. The Cellular and Molecular Basis for Planarian Regeneration. *Cell*. Oct 4  
489 2018;175(2):327-345. <https://doi.org/10.1016/j.cell.2018.09.021>.
- 490 11. Tewari AG, Stern SR, Oderberg IM, Reddien PW. Cellular and Molecular Responses Unique to  
491 Major Injury Are Dispensable for Planarian Regeneration. *Cell Rep*. Nov 27 2018;25(9):2577-2590  
492 e3. <https://doi.org/10.1016/j.celrep.2018.11.004>.
- 493 12. Gavino MA, Wenemoser D, Wang IE, Reddien PW. Tissue absence initiates regeneration through  
494 follistatin-mediated inhibition of activin signaling. *eLife*. Sep 10 2013;2:e00247.  
<https://doi.org/10.7554/eLife.00247>.
- 496 13. Oviedo NJ, Morokuma J, Walentek P, et al. Long-range neural and gap junction protein-  
497 mediated cues control polarity during planarian regeneration. *Dev Biol*. Mar 1 2010;339(1):188-  
498 99. [https://doi.org/S0012-1606\(09\)01402-X](https://doi.org/S0012-1606(09)01402-X) [pii] 10.1016/j.ydbio.2009.12.012.
- 499 14. Thommen A, Werner S, Frank O, et al. Body size-dependent energy storage causes Kleiber's law  
500 scaling of the metabolic rate in planarians. *eLife*. Jan 4 2019;8.  
<https://doi.org/10.7554/eLife.38187>.
- 502 15. Oviedo NJ, Newmark PA, Sanchez Alvarado A. Allometric scaling and proportion regulation in the  
503 freshwater planarian *Schmidtea mediterranea*. *Dev Dyn*. Feb 2003;226(2):326-33.
- 504 16. Wagner DE, Wang IE, Reddien PW. Clonogenic Neoblasts Are Pluripotent Adult Stem Cells That  
505 Underlie Planarian Regeneration. *Science*. May 13 2011;332(6031):811-816.  
<https://doi.org/10.1126/science.1203983>.
- 507 17. Salo E, Baguna J. Cell-Movement in Intact and Regenerating Planarians - Quantitation Using  
508 Chromosomal, Nuclear and Cytoplasmic Markers. *Journal of Embryology and Experimental  
509 Morphology*. 1985;89(Oct):57-70.

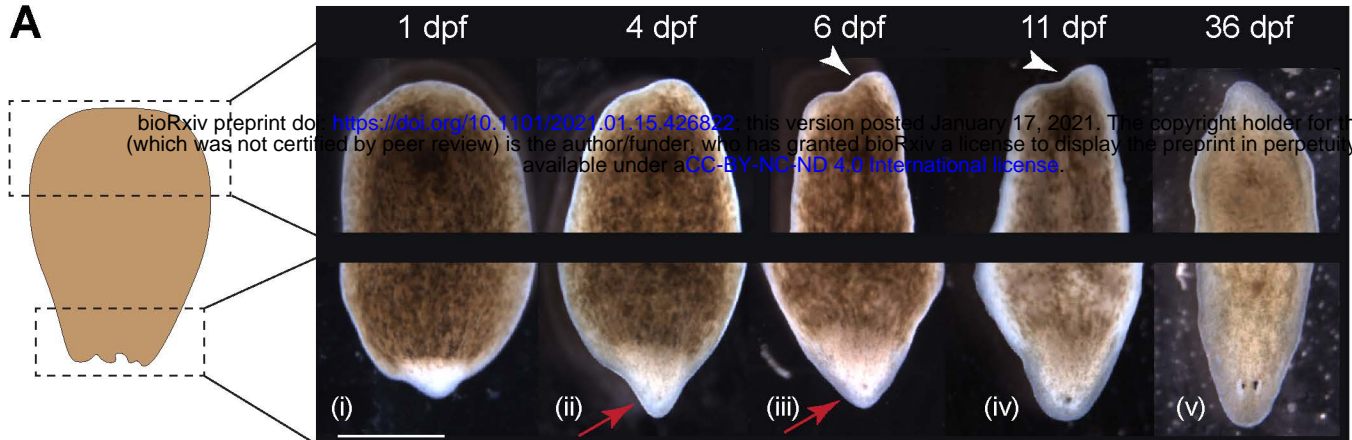
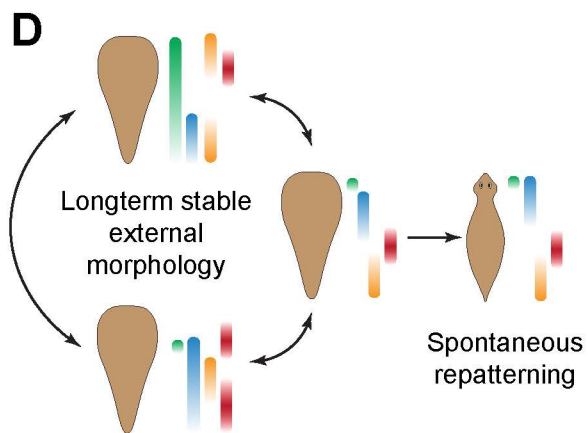
- 510 18. Wenemoser D, Lapan SW, Wilkinson AW, Bell GW, Reddien PW. A molecular wound response  
511 program associated with regeneration initiation in planarians. *Genes Dev.* May 1  
512 2012;26(9):988-1002. <https://doi.org/10.1101/gad.187377.112>.
- 513 19. Agata K, Tasaki J, Nakajima E, Umesono Y. Recent identification of an ERK signal gradient  
514 governing planarian regeneration. *Zoology (Jena)*. Jun 2014;117(3):161-2.  
515 <https://doi.org/10.1016/j.zool.2014.04.001>.
- 516 20. Gurley KA, Elliott SA, Simakov O, Schmidt HA, Holstein TW, Sanchez Alvarado A. Expression of  
517 secreted Wnt pathway components reveals unexpected complexity of the planarian amputation  
518 response. *Dev Biol.* Nov 1 2010;347(1):24-39. <https://doi.org/10.1016/j.ydbio.2010.08.007>.
- 519 21. Wurtzel O, Cote LE, Poirier A, Satija R, Regev A, Reddien PW. A Generic and Cell-Type-Specific  
520 Wound Response Precedes Regeneration in Planarians. *Dev Cell.* Dec 7 2015;35(5):632-645.  
521 <https://doi.org/10.1016/j.devcel.2015.11.004>.
- 522 22. Shin SY, Rath O, Zebisch A, Choo SM, Kolch W, Cho KH. Functional roles of multiple feedback  
523 loops in extracellular signal-regulated kinase and Wnt signaling pathways that regulate  
524 epithelial-mesenchymal transition. *Cancer Res.* Sep 1 2010;70(17):6715-24.  
525 <https://doi.org/10.1158/0008-5472.CAN-10-1377>.
- 526 23. Cebrion F, Nakazawa M, Mineta K, Ikeo K, Gojobori T, Agata K. Dissecting planarian central  
527 nervous system regeneration by the expression of neural-specific genes. *Dev Growth Differ.* Apr  
528 2002;44(2):135-46.
- 529 24. Farinella-Ferruzza N. The transformation of a tail into a limb after xenoplastic transformation.  
530 *Experientia.* 1956;15:304-305.
- 531 25. Gurley KA, Rink JC, Sanchez Alvarado A. b-Catenin Defines Head Versus Tail Identity During  
532 Planarian Regeneration and Homeostasis. *Science.* 2008;319.
- 533 26. Bischof J, Day ME, Miller KA, LaPalme JV, Levin M. Nervous system and tissue polarity  
534 dynamically adapt to new morphologies in planaria. *Dev Biol.* Aug 31 2020.  
535 <https://doi.org/10.1016/j.ydbio.2020.08.009>.
- 536 27. Marsh G, Beams HW. Electrical control of morphogenesis in regenerating *Dugesia tigrina*. I.  
537 Relation of axial polarity to field strength. *J Cell Comp Physiol.* Apr 1952;39(2):191-213.  
538 <https://doi.org/10.1002/jcp.1030390203>.
- 539 28. Adler CE, Seidel CW, McKinney SA, Sanchez Alvarado A. Selective amputation of the pharynx  
540 identifies a FoxA-dependent regeneration program in planaria. *eLife.* Apr 15 2014;3:e02238.  
541 <https://doi.org/10.7554/eLife.02238>.
- 542 29. Witchley JN, Mayer M, Wagner DE, Owen JH, Reddien PW. Muscle cells provide instructions for  
543 planarian regeneration. *Cell Rep.* Aug 29 2013;4(4):633-41.  
544 <https://doi.org/10.1016/j.celrep.2013.07.022>.
- 545 30. Oviedo NJ, Nicolas CL, Adams DS, Levin M. Establishing and maintaining a colony of planarians.  
546 *CSH Protoc.* 2008;2008:pdb prot5053.
- 547 31. Oviedo NJ, Nicolas CL, Adams DS, Levin M. Gene knockdown in planarians using RNA  
548 interference. *CSH Protoc.* 2008;2008:pdb prot5054.
- 549 32. Klagges BRE, Heimbeck G, Godenschwege TA, et al. Invertebrate Synapsins: A Single Gene Codes  
550 for Several Isoforms in *Drosophila*. *The Journal of Neuroscience.* 1996;16(10):3154-3165.  
551 <https://doi.org/10.1523/jneurosci.16-10-03154.1996>.
- 552 33. Rueden CT, Schindelin J, Hiner MC, et al. ImageJ2: ImageJ for the next generation of scientific  
553 image data. *BMC Bioinformatics.* 2017/11/29 2017;18(1):529. <https://doi.org/10.1186/s12859-017-1934-z>.
- 553 34. Schindelin J, Arganda-Carreras I, Frise E, et al. Fiji: an open-source platform for biological-image  
554 analysis [Perspective]. *Nat Methods.* Jun 28 2012;9(7):676-82.  
555 <https://doi.org/10.1038/nmeth.2019>.

558

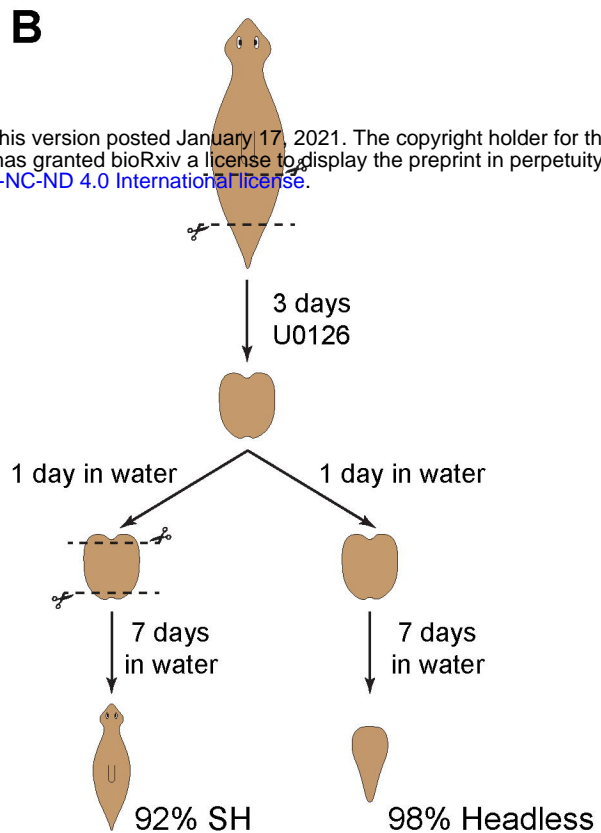
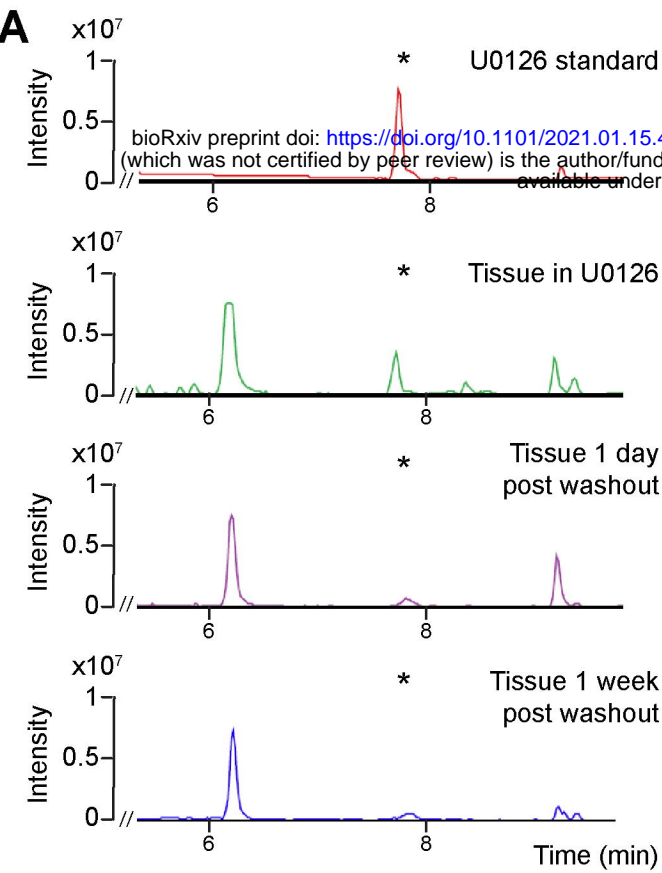


Bischof, et al., Figure 1

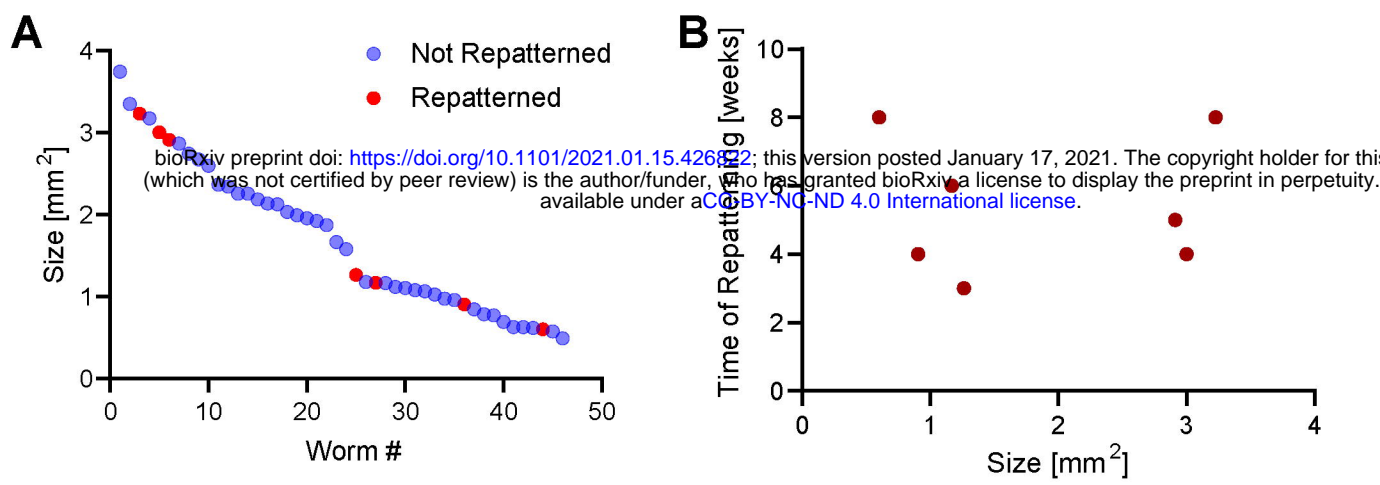
**A****B****C Regeneration Long-term Repatterning****D****E 58 dpa****93 dpa****107 dpa****112 dpa****118 dpa****F****G****H****Bischof, et al., Figure 2**

**A****B****C****D**

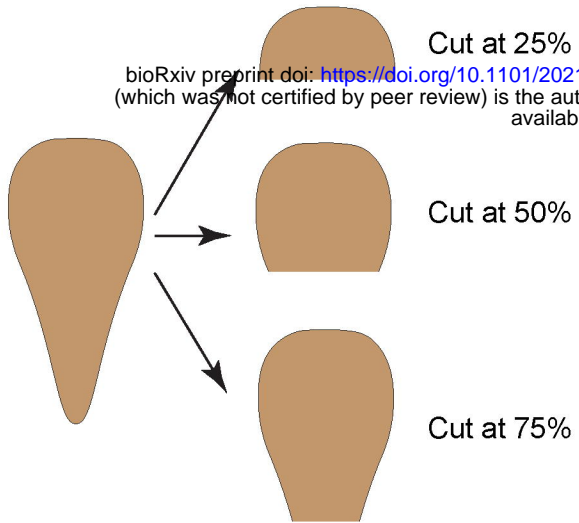
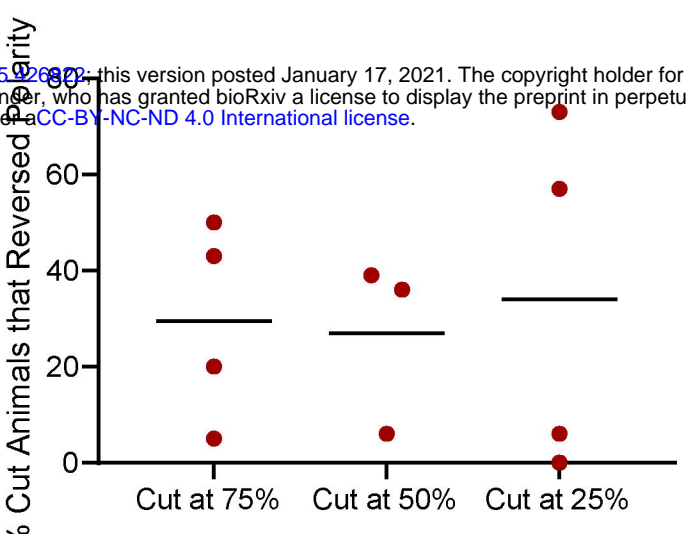
Bischof, et al., Figure 3



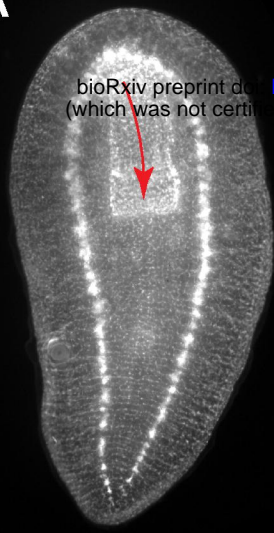
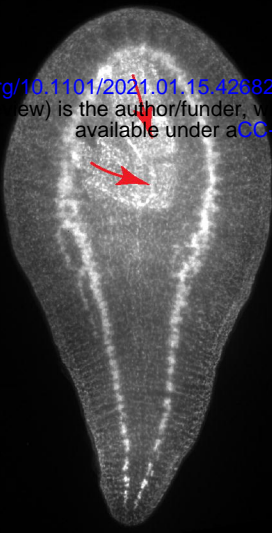
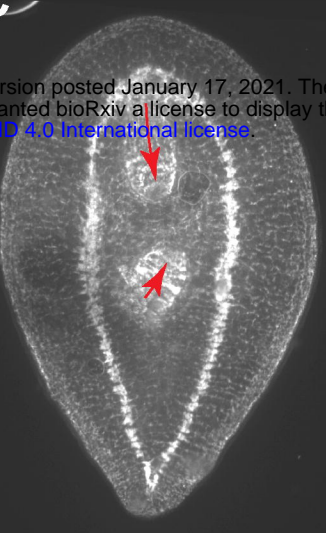
Bischof, et al., Supplemental Figure 1



Bischof, et al., Supplemental Figure 2

**A****B**

Bischof, et al., Supplemental Figure 3

**A****B****C**

bioRxiv preprint doi: <https://doi.org/10.1101/2021.01.15.426822>; this version posted January 17, 2021. The copyright holder for this preprint (which was not certified by peer review) is the author/funder, who has granted bioRxiv a license to display the preprint in perpetuity.

This version posted January 17, 2021. The copyright holder for this preprint (which was not certified by peer review) is the author/funder, who has granted bioRxiv a license to display the preprint in perpetuity. It is made available under aCC-BY-NC-ND 4.0 International license.

Bischof, et al., Supplemental Figure 4